



AIAA-99-0966

**Detonation Solutions from Reactive
Navier-Stokes Equations**

S. Singh, J. M. Powers, and S. Paolucci

Department of Aerospace and Mechanical
Engineering

University of Notre Dame

Notre Dame, Indiana

**37th AIAA Aerospace Sciences
Meeting and Exhibit
January 11-14, 1999 / Reno, NV**

DETONATION SOLUTIONS FROM REACTIVE NAVIER-STOKES EQUATIONS*

Sandeep Singh[†], Joseph M. Powers[‡], and Samuel Paolucci[§],

Department of Aerospace and Mechanical Engineering,
 University of Notre Dame,
 Notre Dame, Indiana 46556-5637.

Abstract

Two-dimensional reactive Navier-Stokes equations are solved using a simple implicit Beam-Warming finite difference scheme. Comparisons of the detonation wave solutions of reactive Euler equations and reactive Navier-Stokes equations show that physical diffusion is important at high resolution when the numerical diffusion becomes negligible. Hence, for accurate detonation wave solutions it is necessary to solve full reactive Navier-Stokes equations which include physical diffusion. High grid resolution and use of physical diffusion enables the use of simple central difference approximations for spatial derivatives. Also, implicit time stepping allows larger time steps relative to explicit schemes at the expense of inversion of a series of block tri-diagonal matrices with small block sizes. Sample problems indicate that by using this method the computations are up to five times faster than the Roe's method, which is commonly used in detonation computations.

Introduction

This study will describe two-dimensional detonation wave solutions of the compressible reactive Navier-Stokes equations. A detonation wave is a strong shock wave propagating in a reactive gas, followed by a thin exothermic reaction zone. The energy of the reaction supports the shock wave. As discussed in detail by Fickett and Davis¹, a steady one-dimensional detonation with a spatially resolved reaction zone structure is known as a ZND wave, named after Zeldovich, von Neumann, and Döring. In experiments² and calculations^{3,4,5} with simplified models it has been observed and predicted that

these ZND waves can be unstable and exhibit a cellular structure in the transverse direction. In experiments², detonation in a tube with walls coated with a thin layer of soot etches detailed regular patterns on the tube walls, indicating the existence of cellular detonation wave structures. For inviscid cases, a normal mode linear stability analysis, in one dimension by Lee and Stewart³, in two dimensions by Short and Stewart⁴ and Clavin, et al.⁶ demonstrates the fundamental instability of the one-dimensional ZND structure to longitudinal and transverse disturbances. Both theoretical and numerical structure of one and two-dimensional detonations has been investigated by Bourlioux, et al.^{7,8} Grismer and Powers⁹ show numerically that detonations which are guaranteed stable in one dimension can be unstable when the geometry is relaxed to include two-dimensional effects. Recently Williams, et al.¹⁰ have shown similar computations for three dimensional geometries. Lastly we note that Clarke, et al.¹¹ have studied the transition to detonation in a viscous gas, but did not consider stability.

Except for Ref. 11, all these calculations are done with reactive Euler equations, and the two dimensional cellular structures turn out to depend on grid resolution, which indicates that numerical diffusion is playing a determining role in predicting the physics. To remedy this, we reintroduce in this study the usually neglected physical mechanisms of mass, momentum and energy diffusion to the conservation equations. It can be shown, as done by Lindström¹², that at low grid resolutions the solutions of both reactive Euler equations and reactive Navier-Stokes equations are similar, because the numerical diffusion dominates over physical diffusion. However, as we increase the grid resolution the numerical diffusion decreases, and physical diffusion becomes important for the accurate solution of reactive Navier-Stokes equations. Hence neglecting physical diffusion at high grid resolution gives rise to non-physical structures in the solutions.

Our main objective is to obtain accurate solutions

* Copyright ©1999 by Sandeep Singh. Published by the American Institute of Aeronautics and Astronautics, Inc. with permission. This study was supported by NSF under CTS-9705150 and AFOSR under F49620-98-1-0206.

[†] Graduate Assistant.

[‡] Associate Professor, Senior Member AIAA.

[§] Associate Professor.

of reactive Navier-Stokes equations. In order to compare with inviscid results, we also include results obtained with a standard Roe's¹³ method solver as applied to reactive Euler equations. In Navier-Stokes simulations, physical diffusion gives rise to smooth solutions, and there is no need to take extraordinary measures, such as embodied in Roe and Flux Corrected Transport (FCT) schemes, in performing spatial discretization. Instead, we use a simple finite difference scheme with second order central differences to model spatial gradients. Use of the central difference approximation for convective terms in the reactive Navier-Stokes equations causes oscillations to develop at the detonation front if the grid resolution is too coarse. However the grid resolution can be made fine enough so that these oscillations disappear. Increasing the grid resolution makes the computations very expensive. Here we exploit the simplicity of the spatial discretization to develop an efficient method to advance the solution in time. We use an implicit method based on the Beam-Warming¹⁴ algorithm. This algorithm uses an Alternating Direction Implicit (ADI) technique based on a linearized trapezoidal time stepping method which is second order accurate in time. The implicit time stepping technique allows use of much larger time steps relative to typical explicit schemes, which have limitations due to convection, diffusion and reaction time scales. Use of larger time steps comes at the expense of a matrix inversion, necessary at every time step. For general systems, this can be prohibitively expensive; however, for reactive Navier-Stokes equations with central difference approximation for spatial gradients and use of the ADI technique we only need to invert block tridiagonal matrices composed of small blocks. Note that it is much less expensive to invert these block tridiagonal systems than general systems. Overall we save on computational time by using this method without any loss of accuracy.

Model Equations

The model equations are taken to be the two dimensional reactive Navier-Stokes equations for a calorically perfect ideal gas. These are expressed in dimensionless form below:

$$\frac{\partial \rho}{\partial t} + \nabla \cdot (\rho \mathbf{u}) = 0, \quad (1)$$

$$\frac{\partial}{\partial t}(\rho \mathbf{u}) + \nabla \cdot (\rho \mathbf{u} \mathbf{u} + P - \tau) = 0, \quad (2)$$

$$\begin{aligned} & \frac{\partial}{\partial t} \left(\rho \left(e + \frac{1}{2} \mathbf{u} \cdot \mathbf{u} \right) \right) + \\ & \nabla \cdot \left(\rho \mathbf{u} \left(e + \frac{1}{2} \mathbf{u} \cdot \mathbf{u} \right) + P \mathbf{u} - \tau \cdot \mathbf{u} + \mathbf{q} \right) = 0, \end{aligned} \quad (3)$$

$$\frac{\partial}{\partial t}(\rho \lambda) + \nabla \cdot (\rho \mathbf{u} \lambda + \mathbf{j}) = \omega, \quad (4)$$

$$\omega = K \rho (1 - \lambda) \exp(-E/T), \quad (5)$$

$$e = \frac{1}{\gamma - 1} \frac{P}{\rho} - \lambda q_0, \quad (6)$$

$$P = \rho T, \quad (7)$$

$$\tau = \mu \left(\nabla \mathbf{u} + \nabla \mathbf{u}^T - \frac{2}{3} (\nabla \cdot \mathbf{u}) \mathbf{I} \right), \quad (8)$$

$$\mathbf{q} = -k \nabla T, \quad (9)$$

$$\mathbf{j} = -D \nabla \rho \lambda. \quad (10)$$

The dependent variables in Eqs. (1-10), ρ , \mathbf{u} , P , T , τ , e , \mathbf{q} , λ , \mathbf{j} , and ω , are the density, velocity vector, pressure, temperature, viscous stress tensor, internal energy per unit mass, heat flux vector, reaction progress variable, mass diffusion flux vector, and reaction source term, respectively. The independent variables are time t and the Cartesian position coordinates x and y , which do not appear explicitly with the vector notation used. The velocity vector components are u and v in x and y directions, respectively. The dimensionless coefficient of viscosity μ , thermal conductivity k , and coefficient of mass diffusion D are respectively

$$\mu = \frac{\sqrt{\gamma}}{Re}, \quad k = \frac{\sqrt{\gamma}}{RePr} \frac{\gamma}{(\gamma - 1)}, \quad D = \frac{\sqrt{\gamma}}{ReSc}. \quad (11)$$

The dimensionless parameters in Eqs. (5-11), q_0 , γ , K , E , Re , Pr , and Sc , are the heat of reaction, ratio of specific heats, kinetic rate constant, activation energy, Reynolds number, Prandtl number, and the Schmidt number, respectively.

Equations (1-3) express conservation principles for mass, momenta, and energy, respectively. Equation (4) is an evolution equation for species mass fraction. A single, first-order, irreversible, exothermic reaction is employed, $A \rightarrow B$. The reaction progress variable λ ranges from zero before reaction to unity

at complete reaction. Species mass fractions, Y_i are related to the reaction progress variable by the formulæ, $Y_A = 1 - \lambda$, $Y_B = \lambda$. Equation (5) defines the reaction source term of Eq. (4) according to the Arrhenius depletion model. Equations (6-7) are caloric and thermal equations of state, respectively. Equation (8) defines the viscous stress as a linear function of the strain rate for an isotropic material which obeys Stokes' assumption. Equations (9-10) express the heat flux and mass diffusion flux by Fourier's and Fick's Laws, respectively. Heat flux due to concentration gradients is neglected along with Dufour and Soret effects.

Density, pressure and temperature are scaled by their constant pre-shock values. Velocities are scaled by a number closely related to the pre-shock acoustic speed. Since a steady, one-dimensional, inviscid ZND wave is chosen as the initial detonation profile, an intrinsic length scale is the half reaction length scale, $\tilde{l}_{1/2}$. It is the distance between the detonation front and the point at which the reaction is halfway to completion, and can be computed by numerical quadrature. The time scale is determined by the velocity and length scales. In terms of dimensional (indicated by the notation "~") variables, parameters, and pre-shock ambient conditions (indicated by the subscript "0"), the dimensionless variables are defined by

$$\begin{aligned} \rho &= \frac{\tilde{\rho}}{\tilde{\rho}_0}, \quad P = \frac{\tilde{P}}{\tilde{P}_0}, \quad T = \frac{\tilde{T}}{\tilde{T}_0}, \\ \mathbf{u} &= \frac{\sqrt{\gamma}}{\tilde{c}_0} \tilde{\mathbf{u}}, \quad e = \frac{\gamma}{\tilde{c}_0^2} \tilde{e}, \quad \tau = \frac{\gamma}{\tilde{P}_0} \tilde{\tau}, \\ \mathbf{q} &= \frac{\sqrt{\gamma}}{\tilde{P}_0 \tilde{c}_0} \tilde{\mathbf{q}}, \quad \mathbf{j} = \frac{\sqrt{\gamma}}{\tilde{\rho}_0 \tilde{c}_0} \tilde{\mathbf{j}}, \quad \omega = \frac{\tilde{l}_{1/2} \sqrt{\gamma}}{\tilde{\rho}_0 \tilde{c}_0} \tilde{\omega}, \\ x &= \frac{\tilde{x}}{\tilde{l}_{1/2}}, \quad y = \frac{\tilde{y}}{\tilde{l}_{1/2}}, \quad t = \frac{\tilde{t}}{\tilde{l}_{1/2} \sqrt{\gamma}} \tilde{t}. \end{aligned} \quad (12)$$

The dimensionless parameters are defined by the following relations:

$$\begin{aligned} q_0 &= \frac{\gamma}{\tilde{c}_0^2} \tilde{q}_0, \quad E = \frac{\gamma}{\tilde{c}_0^2} \tilde{E}, \quad \gamma = \frac{\tilde{c}_p}{\tilde{c}_v}, \\ K &= \frac{\tilde{l}_{1/2} \sqrt{\gamma}}{\tilde{c}_0} \tilde{K}, \quad Re = \frac{\tilde{\rho}_0 \tilde{l}_{1/2} \tilde{c}_0}{\tilde{\mu}}, \quad Pr = \frac{\tilde{\mu} \tilde{c}_p}{\tilde{k}}, \quad (13) \\ Sc &= \frac{\tilde{\mu}}{\tilde{\rho}_0 \tilde{D}_{AB}}, \end{aligned}$$

where the dimensional pre-shock sound speed \tilde{c}_0 and $\tilde{l}_{1/2}$ are given by

$$\tilde{c}_0 = \sqrt{\frac{\gamma \tilde{P}_0}{\tilde{\rho}_0}}, \quad (14)$$

$$\tilde{l}_{1/2} = \tilde{\rho}_0 \tilde{D} \int_0^{1/2} \frac{d\lambda}{\tilde{K} \tilde{\rho}_I(\lambda) (1 - \lambda) \exp(-\tilde{E}/\tilde{T}_I(\lambda))}. \quad (15)$$

Here $\rho_I(\lambda)$ and $T_I(\lambda)$ are functions of the reaction progress variable λ . They can be obtained by solving explicitly for the temperature and density from algebraic Rankine-Hugoniot jump conditions which result in the inviscid limit, represented by the subscript I .

The dimensional parameters are \tilde{q}_0 the heat of reaction, \tilde{E} the activation energy, \tilde{c}_p the specific heat at constant pressure, \tilde{c}_v the specific heat at constant volume, \tilde{K} the kinetic rate constant, $\tilde{\mu}$ the coefficient of viscosity, \tilde{k} the thermal conductivity, \tilde{D}_{AB} the coefficient of species diffusion, and \tilde{D} the steady ZND wave speed.

Numerical Method

In two space dimensions, Eqs. (1-4) can be written as

$$\begin{aligned} \frac{\partial \mathbf{Q}}{\partial t} + \frac{\partial}{\partial x} \left(\mathbf{F}(\mathbf{Q}) - \frac{\partial}{\partial x} (\mathbf{V}_1(\mathbf{Q})) - \mathbf{V}_2(\mathbf{Q}, \mathbf{Q}_x) \right) + \\ \frac{\partial}{\partial y} \left(\mathbf{G}(\mathbf{Q}) - \frac{\partial}{\partial y} (\mathbf{W}_1(\mathbf{Q})) - \mathbf{W}_2(\mathbf{Q}, \mathbf{Q}_x) \right) = \Psi(\mathbf{Q}), \end{aligned} \quad (16)$$

where

$$\begin{aligned} \mathbf{Q} &= \left[\rho, \rho u, \rho v, \rho \left(e + \frac{1}{2}(u^2 + v^2) \right), \rho \lambda \right]^T, \\ \mathbf{F} &= \left[\rho u, \rho u^2 + p, \rho uv, \right. \\ &\quad \left. \rho u \left(e + \frac{1}{2}(u^2 + v^2) + \frac{p}{\rho} \right), \rho u \lambda \right]^T, \\ \mathbf{G} &= \left[\rho v, \rho uv, \rho v^2 + p, \right. \\ &\quad \left. \rho v \left(e + \frac{1}{2}(u^2 + v^2) + \frac{p}{\rho} \right), \rho v \lambda \right]^T, \\ \mathbf{V}_1 &= \left[0, \frac{4}{3} \mu u, \mu v, \right. \\ &\quad \left. \mu \left(\frac{2}{3} u^2 + \frac{1}{2} v^2 \right) + kT, \mathcal{D} \rho z \right]^T, \\ \mathbf{W}_1 &= \left[0, \mu u, \frac{4}{3} \mu v, \right. \end{aligned}$$

$$\begin{aligned} & \mu \left(\frac{1}{2} u^2 + \frac{2}{3} v^2 \right) + kT, \mathcal{D}\rho z \Big]^T, \\ \mathbf{V}_2 &= \left[0, 0, \frac{1}{3} \mu u_y, \mu \left(-\frac{2}{3} uv_y + vu_y \right), 0 \right]^T, \\ \mathbf{W}_2 &= \left[0, \frac{1}{3} \mu v_x, 0, \mu \left(-\frac{2}{3} vu_x + uv_x \right), 0 \right]^T, \\ \Psi &= \left[0, 0, 0, 0, K\rho(1-\lambda) \exp\left(-\frac{E}{T}\right) \right]^T. \end{aligned} \quad (17)$$

Here \mathbf{F} and \mathbf{G} are convective flux vectors in x and y directions, respectively; derivatives of \mathbf{V}_1 , \mathbf{V}_2 , \mathbf{W}_1 , and \mathbf{W}_2 represent the diffusive terms in such a way that mixed derivatives are separated from other second order derivatives; Ψ is the source term vector.

Equation (16) is solved by two methods. The Beam-Warming algorithm is used to solve the reactive Navier-Stokes equations at fine grid resolution. Conservation LAWS PACKage¹⁵ (CLAWPACK) based on Roe's method is used to compare the solutions of reactive Euler equations and reactive Navier-Stokes equations.

Beam-Warming Algorithm

Implicit time stepping is implemented by using Beam-Warming algorithm. The numerical approximation of all the spatial derivatives is done using a second-order central difference approximation. A detailed discussion of the algorithm can be found in Ref. 14. The Beam-Warming algorithm, which is an ADI scheme, is implemented for Eq. (16) in the following three steps:

Step 1:

$$\left(\mathbf{I} + \frac{\theta_1 \Delta t}{1 + \theta_2} \left[\frac{\partial}{\partial x} (\mathbf{A})^n - \frac{\partial^2}{\partial x^2} (\mathbf{R})^n \right] \right) \Delta \mathbf{Q}^* = \Sigma, \quad (18)$$

Step 2:

$$\left(\mathbf{I} + \frac{\theta_1 \Delta t}{1 + \theta_2} \left[\frac{\partial}{\partial y} (\mathbf{B})^n - \frac{\partial^2}{\partial y^2} (\mathbf{S})^n \right] \right) \Delta \mathbf{Q}^n = \Delta \mathbf{Q}^*, \quad (19)$$

Step 3:

$$\mathbf{Q}^{n+1} = \mathbf{Q}^n + \Delta \mathbf{Q}^n, \quad (20)$$

where

$$\begin{aligned} \Sigma &= \frac{\Delta t}{(1 + \theta_2)} \left[\Psi + \frac{\partial}{\partial x} (-\mathbf{F} + \mathbf{V}_1 + \mathbf{V}_2)^n \right. \\ &\quad \left. + \frac{\partial}{\partial y} (-\mathbf{G} + \mathbf{W}_1 + \mathbf{W}_2)^n \right] \end{aligned}$$

$$\begin{aligned} & + \frac{\theta_1 \Delta t}{(1 + \theta_2)} \left[\frac{\partial}{\partial x} (\Delta^{n-1} \mathbf{V}_2) + \frac{\partial}{\partial y} (\Delta^{n-1} \mathbf{W}_2) \right] \\ & + \frac{\theta_2}{(1 + \theta_2)} \Delta \mathbf{Q}^{n-1} \end{aligned} \quad (21)$$

Here $\Delta \mathbf{Q}^n = \mathbf{Q}^{n+1} - \mathbf{Q}^n$. The superscript n refers to the value at time t_n . The time step is given by Δt . The matrices \mathbf{A} , \mathbf{B} , \mathbf{R} and \mathbf{S} are the Jacobian matrices $\partial \mathbf{F} / \partial \mathbf{Q}$, $\partial \mathbf{G} / \partial \mathbf{Q}$, $\partial \mathbf{V}_1 / \partial \mathbf{Q}$ and $\partial \mathbf{W}_1 / \partial \mathbf{Q}$, respectively. The identity matrix is represented by \mathbf{I} . The appropriate choice of the parameters θ_1 and θ_2 , represent various standard difference schemes for time stepping. For example, the fully implicit scheme is given by $\theta_1 = 1$, $\theta_2 = 0$; the trapezoidal scheme is given by $\theta_1 = 1/2$, $\theta_2 = 0$; and the three-point backward scheme is given by $\theta_1 = 1$, $\theta_2 = 1/2$.

The main advantage of using this implicit scheme is that we can take much larger time steps. Although more computational effort is required every time step compared to an explicit scheme, the overall time required to obtain a solution may be less. The extra computational effort is required in solving the block tridiagonal system of linear equations in Eq. (18) which sweeps in the x direction, and in Eq.(19) which sweeps in the y directions, alternately every time step. For two-dimensional reactive Navier-Stokes equations the matrix blocks 5×5 . Another thing to note is that the mixed-derivatives in the viscous terms have been treated explicitly without any loss of accuracy. This is done to preserve the block tridiagonal form of Eqs.(18-19). In this work, we make use of the trapezoidal scheme ($\theta_1 = 1/2$, $\theta_2 = 0$) which yields second-order temporal accuracy in our calculations.

Roe's Method

Roe's method is a general technique for discretizing hyperbolic conservation laws. One of its attractive features is its ability to capture discontinuities within a small number of computational cells while minimizing spurious oscillations which arise from numerical discretization. We use the CLAWPACK routines to implement Roe's method. CLAWPACK is a general package of Fortran 77 subroutines for solving time-dependent systems of conservation laws in one, two and three dimensions. The multidimensional algorithms used in CLAWPACK are primarily the extension of one-dimensional wave propagation methods described in detail by LeVeque¹⁶. The algorithms are based upon upwind Godunov's¹⁷ method and require the exact or approximate solution of a Riemann problem at computational cell interfaces in order to advance the solution in time. Our equations, with the

initial condition of an inviscid ZND wave, admit discontinuous solutions, which are captured effectively and oscillation free using CLAWPACK without resorting to artificial dissipation even at coarse grid resolutions.

Equation (16) is numerically solved on the computational grid using the method of fractional steps by Strang¹⁸

$$\mathbf{Q}^{n+1} = \mathcal{L}_{s+v}^{\Delta t/2} \mathcal{L}_c^{\Delta t} \mathcal{L}_{s+v}^{\Delta t/2} \mathbf{Q}^n, \quad (22)$$

where \mathbf{Q}^{n+1} and \mathbf{Q}^n are numerical approximations for \mathbf{Q} at the times $t_n + \Delta t$ and t_n ($t_n = n\Delta t$), respectively. With subscripts c for convection, s for source, and v for viscous terms, respectively, $\mathcal{L}_c^{\Delta t}$ and $\mathcal{L}_{s+v}^{\Delta t}$ are the solution operators for Eq. (23) and Eq. (24), respectively:

$$\frac{\partial \mathbf{Q}}{\partial t} + \frac{\partial}{\partial x}(\mathbf{F}(\mathbf{Q})) + \frac{\partial}{\partial y}(\mathbf{G}(\mathbf{Q})) = 0, \quad (23)$$

$$\begin{aligned} & \frac{\partial \mathbf{Q}}{\partial t} + \frac{\partial}{\partial x} \left(-\frac{\partial}{\partial x}(\mathbf{V}_1(\mathbf{Q})) - \mathbf{V}_2(\mathbf{Q}, \mathbf{Q}_y) \right) \\ & + \frac{\partial}{\partial y} \left(-\frac{\partial}{\partial y}(\mathbf{W}_1(\mathbf{Q})) - \mathbf{W}_2(\mathbf{Q}, \mathbf{Q}_x) \right) = \Psi(\mathbf{Q}). \end{aligned} \quad (24)$$

Strang splitting retains second-order temporal accuracy if individual time steps have second-order temporal accuracy. The time interval Δt is chosen based upon the following stability conditions

$$\Delta t = \min \left[\frac{(CFL)\Delta x}{(|u| + c)_{max}}, \frac{(CFL)\Delta y}{(|v| + c)_{max}}, \frac{\rho_{min}\Delta x^2}{2\delta}, \frac{\rho_{min}\Delta y^2}{2\delta} \right] \quad (25)$$

where ρ , u , v and c are density, velocity components in x and y directions, and the sound speed, respectively. The grid spacings in x and y directions are given by Δx and Δy . The subscripts max and min refer to the respective maximum and minimum values in the computational domain. CFL is the Courant-Friedrichs-Lewy number which is chosen to be 0.4 in our computations. The largest diffusion coefficient is $\delta = \max[\mu, k, D]$. The smallest Δt obtained from the above constraints is used as the time interval at every time step.

CLAWPACK is used to solve the convective step in Eq. (23). The approximate Riemann solver used for our problem is Roe's¹³ solver. The numerical approximation of the convective fluxes at the cell interfaces, is determined from the approximate solution of the

Riemann problem. Second-order spatial accuracy is obtained as a correction to the fluxes, based on standard flux-limiter methods. The other flux corrections employed are for "entropy fix" of any transonic rarefaction wave, transverse wave propagations and their second-order corrections, and transverse propagation of the second order corrections. These are discussed in detail by LeVeque¹⁶. The second-order temporal accuracy is achieved by a predictor/corrector Runge-Kutta integration.

Before and at the end of each convective step CLAWPACK calls a subroutine where the source and viscous terms are solved for explicitly as in Eq. (24). For the reactive Euler equations the viscous terms are neglected. Central difference approximation of second-order is used for the numerical approximation of the viscous terms. Again second-order Runge-Kutta integration is used for second-order temporal accuracy.

Results and Discussion

In our numerical study, we consider a detonation wave propagating in an infinite width rectangular channel. The initial state is taken to be the steady solution of the one-dimensional reactive Euler equations. The initial one-dimensional profile is spatially perturbed in the transverse direction. The perturbation is sinusoidal with a wavelength equal to that predicted by Short and Stewart⁴ for a case in which only one unstable mode was found in their linear stability analysis. Since periodic perturbations are used, periodic boundary conditions are imposed in the direction transverse to the direction of wave propagation. Our computational domain is of finite length and is translated every time step in such a way that the rightmost 15% of the domain contains only gas which is essentially unreacted. This is done in order to prevent the detonation wave from traveling out of the computational domain. The boundary conditions imposed at left and right side of the computational domain are fixed and are same as the left and right states of the initial inviscid ZND wave.

We choose parameters equivalent to those of Short and Stewart⁴. The non-dimensional heat release parameter q_0 and activation energy E are taken to be 50, and the ratio of specific heats γ is taken to be 6/5. The dimensional parameters were chosen to be $\bar{P}_0 = 10^5$ Pa, $\bar{\rho}_0 = 1.161$ kg/m³, $\bar{T}_0 = 300$ K, $\bar{q}_0 = 4.305 \times 10^8$ J/kg, $\bar{E} = 4.305 \times 10^8$ J/kg, $\bar{c}_p = 1722$ J/(kg K), $\bar{c}_v = 1435$ J/(kg K), $\bar{K} = 1.329 \times 10^7$ s⁻¹, $\bar{\mu} = 1.846 \times 10^{-5}$ (N-s)/m, $\bar{k} = 3.179 \times 10^{-2}$ (N-m)/(s-K), $\bar{D}_{ab} = 1.590 \times 10^{-5}$ m²/s, and $\bar{D} = 2.963 \times 10^3$ m/s. The coefficient of viscosity $\bar{\mu}$ is chosen to be

that of air at 300 K. The thermal conductivity \bar{k} is chosen by taking the Prandtl number Pr to be 1. The diffusion coefficient \bar{D}_{ab} is chosen to render the Schmidt number Sc to be 1. Consequently, the Lewis number, $Le = Sc/Pr$, is also 1. With these choices the dimensionless transport coefficients take on the values $\mu = 0.01$, $k = 0.06$, and $\mathcal{D} = 0.01$. The steady ZND wave speed \bar{D} is chosen such that the square of the ratio of \bar{D} to the Chapman Jouguet speed \bar{D}_{CJ} , defined as the overdrive factor $f = (\bar{D}/\bar{D}_{CJ})^2$, has a value of $f = 2.2$. The half reaction length scale $\bar{l}_{1/2}$ is 5.416×10^{-6} m and the sound speed \bar{c}_0 is 321.4 m/s for the given parameters. This determines the remaining non-dimensional parameters, the reaction constant $K = 72$ and the Reynolds number $Re = 109.5$. The initial ZND profile based on the above parameters is shown in Fig. 1.

The wavelength of the transverse disturbance is chosen based on the study by Short and Stewart⁴, in which it is shown that for $f = 2.2$ and $q_0 = E = 50$, there is only a single mode of instability present in the ZND wave. A wavelength of slightly less than 10 has the maximum growth rate of the instability and hence emerges as the dominant feature as regular detonation cells of size 10 in two-dimensional detonations. Bourlioux and Majda⁸ have done computations for the similar case for the reactive Euler equations. Hence our computational domain is chosen to have $0 \leq y \leq 10$. We also choose a local domain length in the x direction of 14; this domain propagates with the wave. The shock front of the initial ZND wave is positioned at $x = 12$ as seen in Fig. 1.

The computations are done for varying grid resolutions. In all calculations, the computational cells are square. The grid resolutions used are 2, 5, 12, 19 and 24 grid points for every half reaction length scales, as predicted by inviscid theory. At fine grid resolutions of 1/12, 1/19 and 1/24, the computations for reactive Navier-Stokes equations are done with the Beam-Warming method when the oscillations due to the use of central difference approximations are minimal. Roe's method is used to compare the solutions of reactive Euler equations and reactive Navier-Stokes equations at the grid resolutions of 1/2, 1/5, and 1/12. All the calculations are done on a Sun Ultra 30 workstation. The highest resolution case, solved with the Beam-Warming method, takes approximately 30 hours to solve.

First the comparison between the reactive Euler equations and the reactive Navier Stokes equations are presented. All figures show a contour plot of isochoric lines for the values of $\rho = 1, 1.25, 1.5, 1.75, \dots$. Figures (2a - 2c) depict the solutions of reactive Euler

equations for increasing grid resolutions at times $t = 40, 80, 120$. Figures (3a - 3c) depict the solutions of reactive Navier-Stokes equations using Roe's method for increasing grid resolutions at times $t = 40, 80, 120$. We observe familiar structures of regular detonation cells. The cell size is found to be same as the transverse wavelength. Computations, not shown here, were also done for a domain width of $0 \leq y \leq 20$, which still generated cellular structures of size of the order of 10. Hence we compute for a domain width of 10 and show it twice in our results.

It is found that the results are similar at a coarse grid resolution of 1/2 for both reactive Euler equations and reactive Navier-Stokes equations. For higher grid resolutions of 1/5 and 1/12, we predict that the solutions of reactive Euler equations and reactive Navier-Stokes equations are very different. As we increase the grid resolution we observe that more and more fine structures are predicted by the Euler model, thereby we conclude that the two-dimensional cellular structures in reactive Euler equations depend on the grid resolution. However, as we increase the grid resolution, the predictions of the Navier-Stokes equations using Roe's method appear to converge. The reactive Navier-Stokes equations have two physical length scales associated with them: a relatively large length scale associated with the reaction zone and a relatively small diffusion length scale which is of the order of 1/5 half reaction length scale. For a coarse grid size of 1/2, the diffusion length scale is completely unresolved and the numerical diffusion dominates over the physical diffusion making the reactive Euler and reactive Navier-Stokes solutions appear similar. But for finer grid sizes of 1/5 and 1/12, as the viscous length scales are resolved, the reactive Euler and reactive Navier-Stokes solutions begin to differ. Hence as we go to higher resolutions, both the viscous and reaction zone length scales are resolved simultaneously, and the solution of the reactive Navier-Stokes equations using Roe's method appears to converge.

Figures (4a - 4c) depict the solutions of reactive Navier-Stokes at fine grid sizes of 1/12, 1/19 and 1/24 obtained by the Beam-Warming method. Again we can see the solution appears to converge as we increase the grid resolution. There appear to be some oscillations for the grid size 1/12 but for the grid sizes 1/19 and 1/24 the oscillations are non-existent. Also the comparison between Fig. 3c and Fig. 4a, which are the solutions of reactive Navier Stokes equations by Roe's method and Beam-Warming method, respectively, at same grid resolution of 1/12, shows that the two methods yield identical results. The time steps taken in these computations were up to ten

times more than the time steps taken in the explicit methods due to their relaxed stability restrictions. The main advantage of using this method was that for the cases run, this method was up to five times faster than the Roe's method. In fact the run time for the Beam-Warming method at the grid resolution 1/19 was same as the run time of Roe's method at grid resolution of 1/12. The convergence of the solution as grid resolution is increased was also better.

Summary

Our numerical study of reactive Navier-Stokes equations has shown the importance of the physical diffusion terms for detonation wave solutions. At fine grid resolutions, when the numerical diffusion becomes negligible, we predict non-physical structures appearing in the solution of reactive Euler equations. Hence it became necessary to solve the full reactive Navier-Stokes equations for true detonation wave solutions. We have also shown that the grid size should be small enough to resolve both length scales associated with chemistry and physical diffusion. Due to the requirement of small grid sizes, we used simple central differences to approximate spatial gradients as the oscillations are minimal for very high resolutions. Finally an efficient Alternating Direction Implicit scheme of Beam-Warming was used to advance in time. This reduced the computational time by up to five times, relative to Roe's method conventionally used for detonation solutions, while preserving accuracy. Subsequently, such elaborate and computationally expensive upwind schemes are not necessary.

References

- ¹Fickett, W., and Davis, W. C., *Detonation*, University of California Press, Berkeley, 1979.
- ²Strehlow, R. A., and Fernandes, F. D., *Combustion and Flame*, Vol. 9, 1965, pp. 31-58.
- ³Lee, H. I., and Stewart, D. S., "Calculation of Linear Detonation Instability: One-Dimensional Instability of Plane Detonation," *Journal of Fluid Mechanics*, Vol. 216, 1990, pp. 103-132.
- ⁴Short, M., and Stewart, D. S., "Cellular Detonation Stability. Part 1. A Normal-Mode Linear Analysis," *Journal of Fluid Mechanics*, Vol. 368, 1998, pp. 229-262.
- ⁵Erpenbeck, J. J., "Nonlinear Theory of Two-Dimensional Detonations," *The Physics of Fluids*, Vol. 13, 1970, pp. 2007-2026.
- ⁶Clavin, P., He, L., and Williams, F. A., "Multidimensional Stability Analysis of Overdriven Gaseous Detonations," *Physics of Fluids*, Vol. 9, No. 12, 1997, pp. 3764-3785.

⁷Bourlioux, A., Majda, A. J., and Roytburd, V. "Theoretical and Numerical Structure for Unstable One-Dimensional Detonations," *SIAM Journal of Applied Mathematics*, Vol. 51, No. 2, 1991, pp. 303-343.

⁸Bourlioux, A., and Majda, A. J., "Theoretical and Numerical Structure for Unstable Two-Dimensional Detonations," *Combustion and Flame*, Vol. 90, 1992, pp. 211-229.

⁹Grismer, M. J., and Powers, J. M., "Numerical Predictions of Oblique Detonation Stability Boundaries," *Shock Waves*, Vol. 6, 1996, pp. 147-156.

¹⁰Williams, D. N., Bauwens, L., and Oran, E. S., "Detailed Structure and Propagation of Three-Dimensional Detonations," *Twenty-Sixth Symposium (International) on Combustion*, The Combustion Institute, Pittsburgh, 1996.

¹¹Clarke, J. F., Kassoy, D. R., Meharzi, N. E., Riley, N., Vasantha, R., "On the Evolution of Plane Detonations," *Proceedings of the Royal Society of London Series A*, Vol. 429, 1990, pp. 259-283.

¹²Lindström D., "Numerical Computation of Viscous Detonation Waves in Two Space Dimensions," Department of Scientific Computing, Uppsala University, 1996.

¹³Roe, P. L., "Approximate Riemann Solvers, Parameter Vectors, and Difference Schemes," *Journal of Computational Physics*, Vol. 43, No. 2, 1981, pp. 357-372.

¹⁴Anderson, D. A., Tannehill, J. C., and Pletcher, R. H., *Computational Fluid Mechanics and Heat Transfer*, Hemisphere Publishing Corporation, 1984.

¹⁵LeVeque, R. J., "Wave Propagation Algorithms for Multi-Dimensional Hyperbolic Systems," *Journal of Computational Physics*, Vol. 131, 1997, pp. 327-353.

¹⁶LeVeque, R. J., *Numerical Methods for Conservation Laws*, Birkhäuser Verlag, Boston, 2nd edition, 1992.

¹⁷Godunov, S. K., "A Difference Scheme for Numerical Computation of Discontinuous Solution of Hydrodynamic Equations," *Sbornik Mathematics*, Vol. 47, 1959, pp. 271-306.

¹⁸Strang, G., "On the Construction and Comparison of Difference Schemes," *SIAM Journal on Numerical Analysis*, Vol. 5, 1968, pp. 506-517.

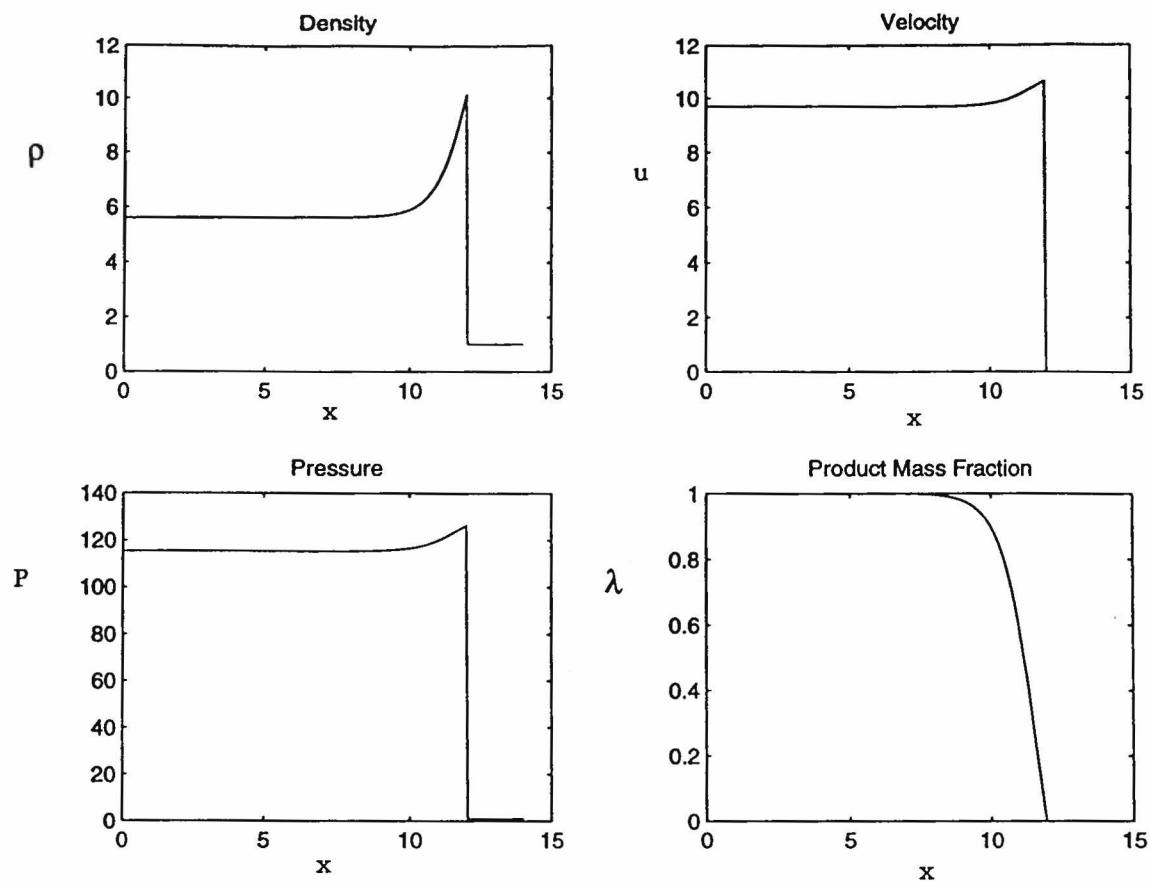


Figure 1: Inviscid ZND profiles for density, velocity, pressure and mass fraction used as initial conditions for viscous calculations.

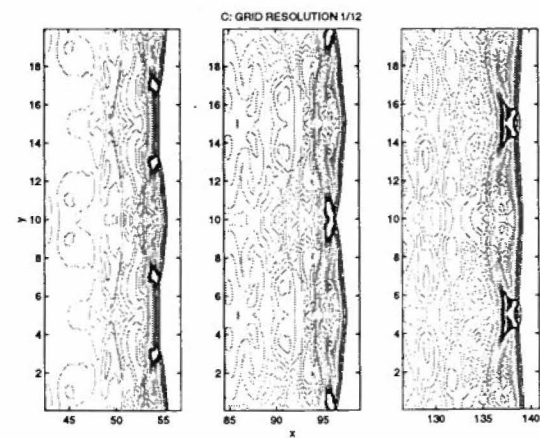
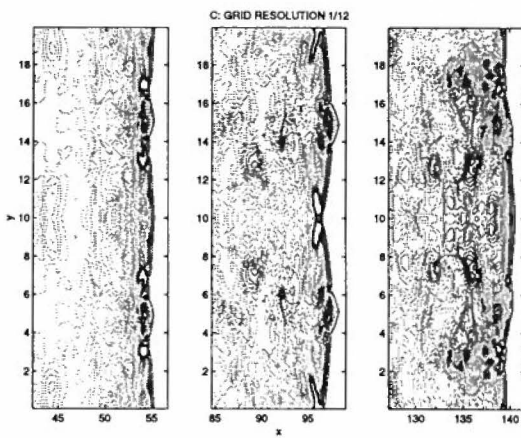
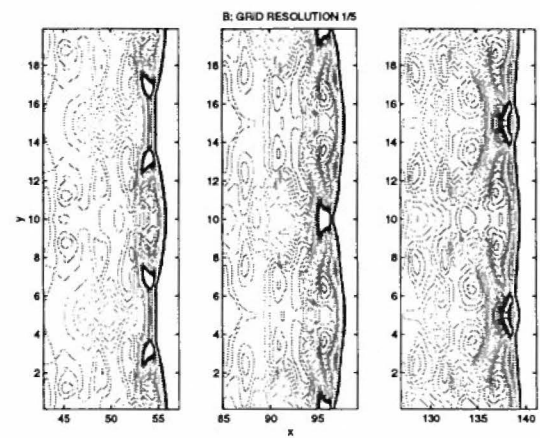
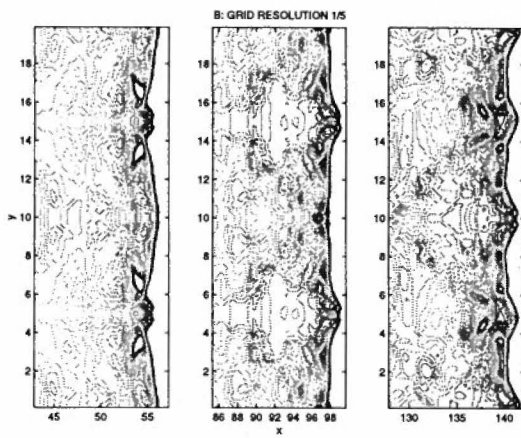
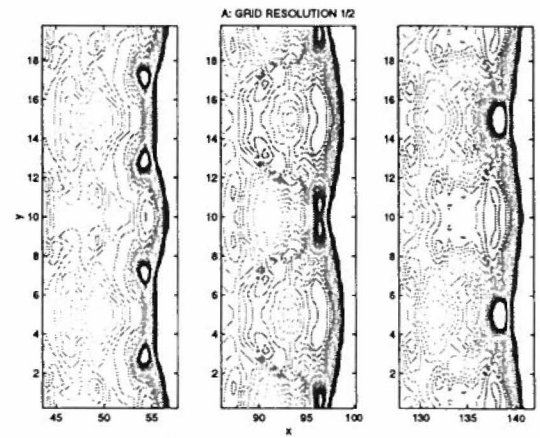
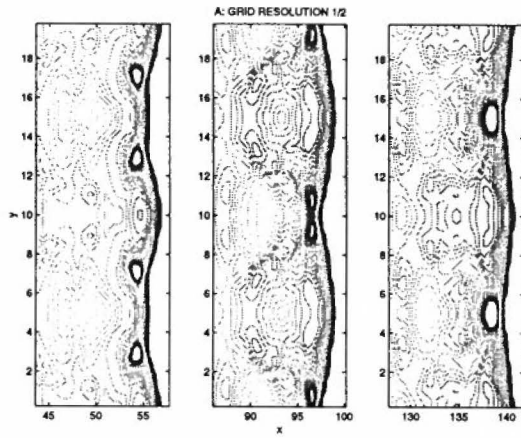


Figure 2: Isochoric lines for the solutions of reactive Euler equations at times $t = 40, 80,$ and 120 ; using Roe's method.

Figure 3: Isochoric lines for the solutions of reactive N-S equations at times $t = 40, 80,$ and 120 ; using Roe's method.

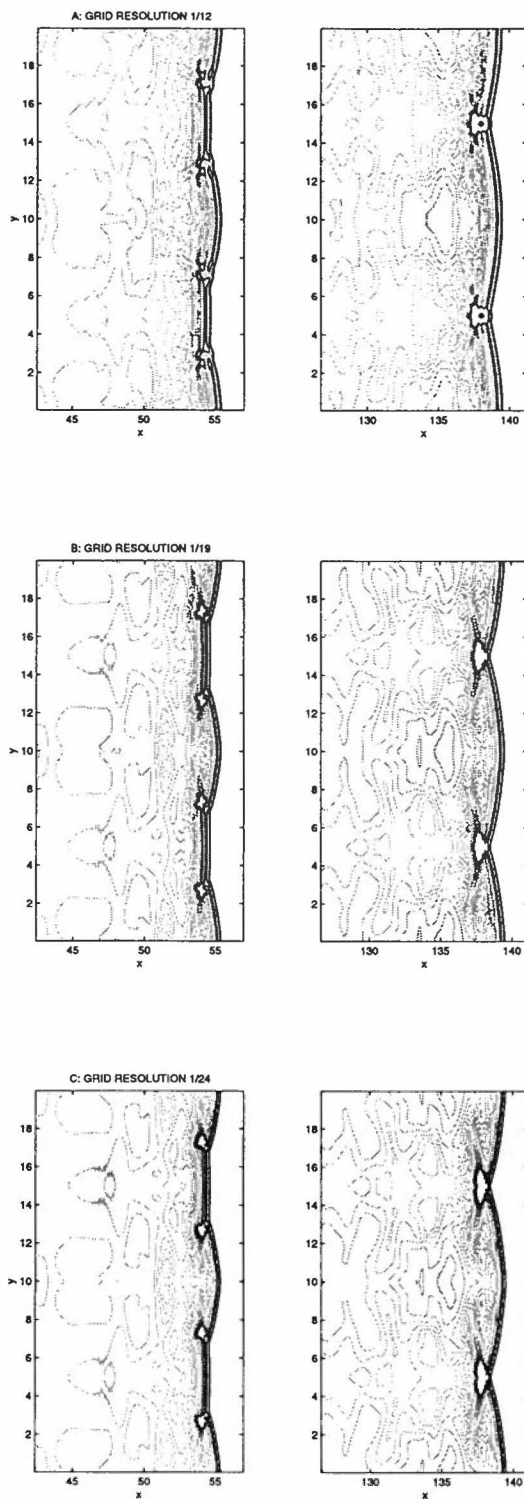


Figure 4: Isochoric lines for the solutions of reactive N-S equations at times $t = 40$, and 120 ; using Beam-Warming method.

